Analysis of the TOF single-channel performance by using cosmic rays triggered in the ALICE experiment during the 2016/17 data taking campaign

Zuzana Moravcová, Czech Technical University in Prague, Czech republic
under the supervision of
Manuel Colocci, University and INFN Bologna, Italy

***Abstract*—The ALICE Time-Of-Flight detector has well defined time resolution of 56 ps for the beam data. In this work project report, the analysis of cosmic rays is presented with the focus on receiving the time resolution for different levels of granularity of TOF. The obtained value ($\sim$ 90 ps if there is a sufficient statistics) is uniform through different momentum bins, geometry of the detector and readout electronics as well.**

I. Time-Of-Flight detector

ALICE, or A Large Ion Collider Experiment, is a heave-ion experiment situated at Point 2 of the Large Hadron Collider (LHC). Its main physical goal is to study proprieties of Quark Gluon Plasma (QGP), a state of hot and dense matter which existed a few microseconds after the Big Bang where quarks and gluons existed without confinement. QGP is created at LHC by colliding heavy nuclei at TeV energies.

Since thousands of particles are created in this kind of collision, a particle identification (PID) with high reliability is crucial. On ALICE, several methods are used for PID, such as:

- Specific energy loss ($^{dE}/_{dx}$) measurement by Time Projection Chamber (TPC)
- Transition radiation measurement by Transition Radiation Detector (TRD)
- Time of flight of particles measurement by Time-Of-Flight detector (TOF)

Most of the analysis made with ALICE are using a combination of the mentioned techniques.

The TOF detector, located 3.7 - 4.0 m away from the beam pipe and based on Multigap Resistive Plate Chamber (MRPC) technology, is important to identify different types of hadrons. With its cylindrical shape, it has 2π azimuthal and $|\eta| < 0.9$ polar acceptance. The large active area (S = 141 m^2) is divided into 18 supermodules (SM). Each contains 5 modules with either 15 (central) or 19 (others) MRPCs which makes 91 MRPCs (strips) for each SM. Each strip can be further divided into 4 front-end analytics (FEA) which is made from 24 channels. In total, TOF is made from 152928 readout channels.

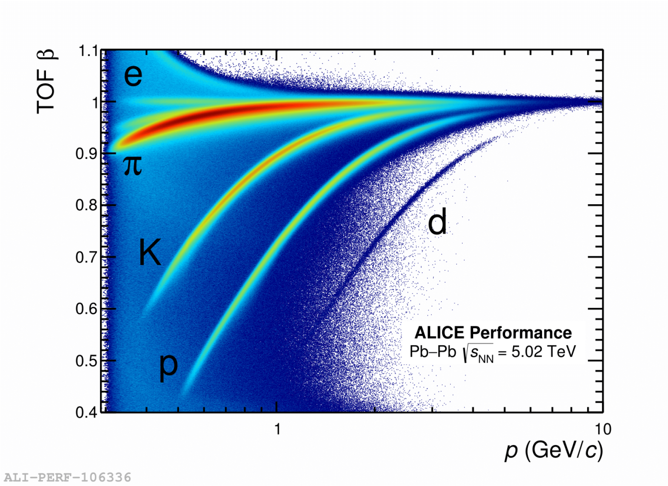

Fig. 1: Velocity of particle ($\beta = {}^{v}/_{c}$) measured by the TOF as a function of momentum p in Pb-Pb collisions at $\sqrt{s_{\rm NN}} = 5.02$ TeV. Taken from [1].

II. TOF time resolution – beam data

Since Run 2, TOF is capable to distinguish between π/K and p/K up to 3 GeV/c and 5 GeV/c, respectively.[1] This capacity is shown on Fig. 1 based on $\beta = v/c$. Forasmuch as PID depends on a time resolution of TOF, it is crucial to have the best possible one. In Run 1, the time resolution was 84 ps. Thanks to 2017 calibration, present time resolution of 56 ps can be found on Fig. 2. This resolution ($\sigma_{\rm TOT}$) is obtained as

$$\begin{aligned}\sigma^2_{\rm TOT} &= \sigma^2_{\rm TOF} + \sigma^2_{\rm trk} + \sigma^2_{\rm event} \quad (1)\\ &= \sigma^2_{\rm MRPC} + 2\ \sigma^2_{\rm TDC} + \sigma^2_{\rm FEE} + \sigma^2_{\rm clock} + \sigma^2_{\rm Cal} + \sigma^2_{\rm trk} + \sigma^2_{\rm event},\end{aligned}$$

where $\sigma_{\rm trk}$ is the tracking particle uncertainties, $\sigma_{\rm event}$ is the resolution on the event time, $\sigma_{\rm MRPC}$ is the MRPC intrinsic resolution, $\sigma_{\rm TDC}$($\sim$20 ps) and $\sigma_{\rm FEE}$($\sim$10 ps) is the readout and front-end electronic time resolution, respectively, $\sigma_{\rm clock}$($\sim$15 ps) is the LHC clock, and $\sigma_{\rm Cal}$ is the calibration time resolution [1].

The gained resolution (56 ps) is from beam data (Pb-Pb collisions at $\sqrt{s_{\rm NN}} = 5.02$ TeV) for fixed momentum ($p = 1.5$ GeV/c) where good particle separation is possible.

[1]For Run 1, π/K separation was possible up to 2.5 GeV/c while p/K up to 4 GeV/c.

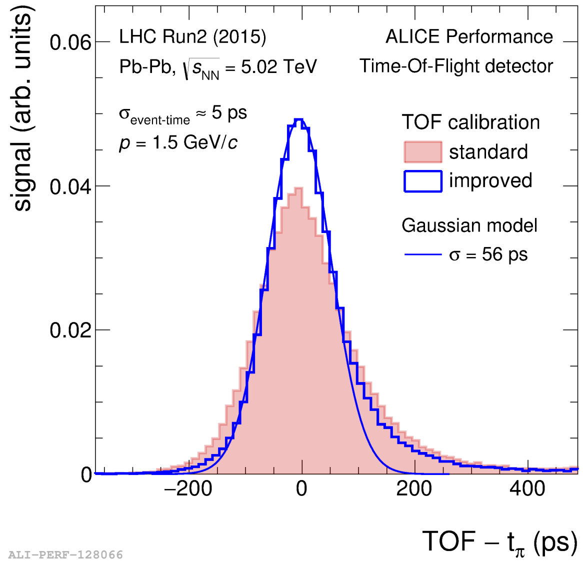

Fig. 2: TOF time resolution in Pb-Pb collisions at $\sqrt{s_{NN}} = 5.02$ TeV. Taken from [1].

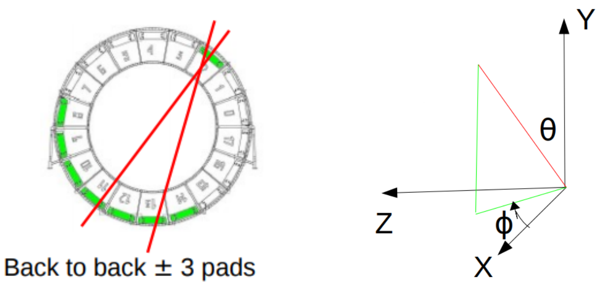

(a) OB3 trigger.

(b) Axis labelling.

Fig. 3: Back-to-back track cuts scheme. Taken from [2].

With sufficient statistics, it is achievable to obtain time resolution for different levels of granularity of TOF, from sectors to the single-channel level and check the stability of TOF performance. We decided to use cosmic muons for this kind of analysis because compared to beam data cosmic events are much clearer (almost no background).

III. Event selection

From cosmic rays data taking campaign from 2015 to 2017, we used for this analysis following runs (all with $B = 0.5$ T): 246469, 273789, 273999, 274041, 274295, 274429, 275878, 276817, 276825, 276871, 276950, 279803, 279804, 281375, with 7.6 millions OB3 triggered events in total. Run number 275878 (with 1.4M events) was used as a test run.

We had several requirements on cited events. First, we observed events with precisely two tracks with extra conditions to be sure those tracks are from one particle:

- Trigger includes OB3 – when cosmic particle hits the TOF, the opposite supermodule $\pm$ 3 pads are turned on (see Fig. 3a).
- When z is the axis along the beam pipe and y is pointing to the top of the detector, we denote θ and ϕ angles between axis as shown on Fig. 3b (θ in the plane yz, $0 \leq \theta < \pi$, and ϕ in the plane xy, $0 \leq \phi < 2\pi$). Then in ideal case of back-to-back tracks, the position of hits of cosmics should follow the conditions $\Delta\phi = \phi_2 - \phi_1 = \pi$ and $\sum\theta = \theta_1 + \theta_2 = \pi$. Distribution of $\Delta\phi$ and $\sum\theta$ before cuts is shown on Fig. 4. The two-dimensional histogram was subsequently fitted with 2D Gaussian (with fixed mean at (π, π)), the obtained σ was finally used to choose the final cut (3σ in both dimensions as shown on Fig. 5 with red dashed lines.)
- The closest points (to each other) of two recorded tracks have coordinates (x_1, y_1, z_1) and (x_2, y_2, z_2), respectively. Differences of those points ($\Delta x = x_1 - x_2$ and $\Delta y = y_1 - y_2$) are shown at Fig. 6 together with 3σ cuts obtained in the same way as the previous cuts (2D Gaussian with fixed mean at $(0, 0)$).

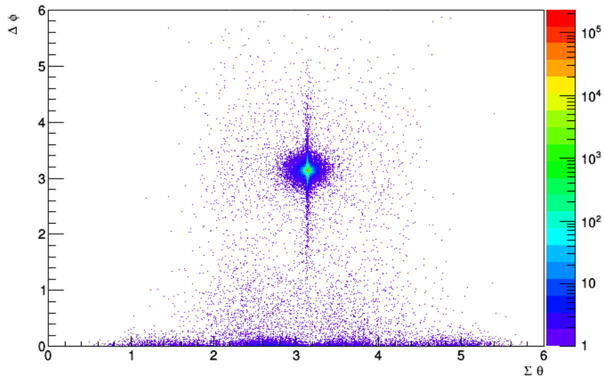

Fig. 4: Distribution of $\Delta\phi$ and $\sum\theta$ before cuts.

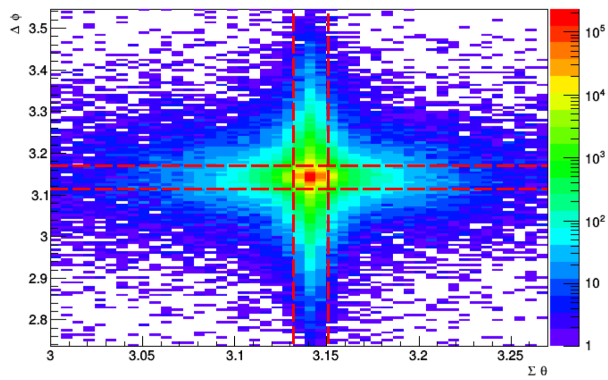

Fig. 5: Distribution of $\Delta\phi$ and $\sum\theta$ shown with 3σ cut (red dashed line).

Momentum cut ($p > 2$ GeV/c) was necessary to allow us to work with a straight line approximation instead of real trajectories. Relative error between those variables, shown on Fig. 7 as a function of transverse momentum, was computed as

$$\frac{R \cdot \arcsin(L/2R) - L/2}{R \cdot \arcsin(L/2R)}, \tag{2}$$

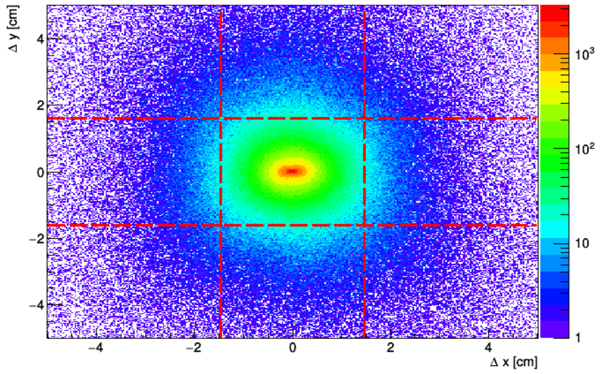

Fig. 6: Distribution of Δx and Δy shown with 3σ cut (red dashed line).

where L is the length of straight line between two hits in TOF and R is radius of the circle on which the charged particle in the magnetic field ($B = 0.5$ T in ALICE) is moving deduced from the formula

$$R = \frac{p_{\mathrm{T}}}{0.3 \cdot B}. \tag{3}$$

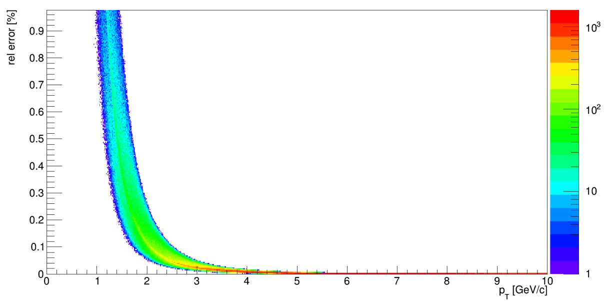

Fig. 7: Relative error between straight line approximation and real particle trajectory as a function of transverse momentum.

Last but not least, we had a cut on pseudorapidity ($|\eta| < 0.8$) because of the geometry of the detector and we required both hits at TOF.

Summary of chosen cuts and how many events passed through each cut is shown on Fig. 8.

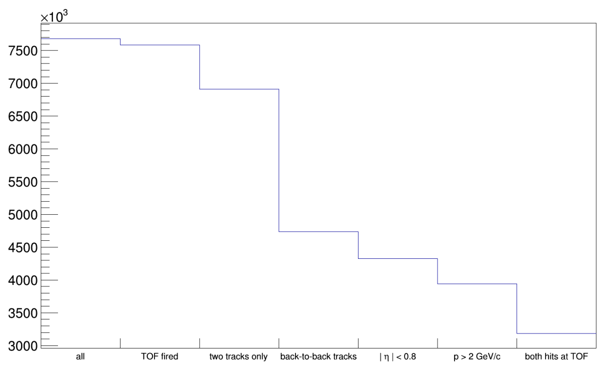

Fig. 8: Event selection statistics.

IV. TOF TIME RESOLUTION – COSMICS

The first difference between obtaining a time resolution from beam data and from cosmics is that during the beam data, we rely on one time recorded by TOF[2] while in cosmics data both times are obtained from the hit in TOF. The resolution in that case is not σ from fitting with a Gaussian by $\sigma/\sqrt{2}$.

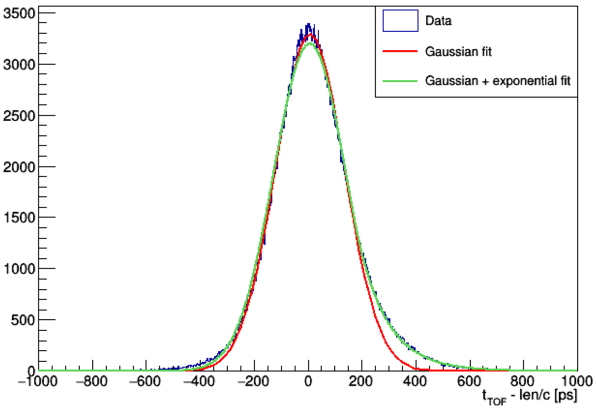

Fig. 9: Distribution of $t_{\mathrm{TOF}} - L/c$ for particles with $p > 2$ GeV/c.

The distribution of $t_{\mathrm{TOF}} - L/c$, where t_{TOF} is the time difference between two hits in TOF, is shown at Fig. 9. The histogram was fitted with a Gaussian (red) and with a function

$$\begin{aligned} f(x) &= \exp\left(-\frac{(x-\langle x\rangle)^2}{2\sigma^2}\right) && \text{for } x < \langle x\rangle + \tau\cdot\sigma \\ f(x) &= \exp\left(-(x-\langle x\rangle - \frac{\tau\cdot\sigma}{2})\frac{\tau}{\sigma}\right) && \text{for } x > \langle x\rangle + \tau\cdot\sigma, \end{aligned} \tag{4}$$

referred as a Gaussian + exponential. The obtained parameters of two fits are in Table I.

Gaussian:

$\langle x\rangle$	-3.8 ± 0.2
σ	120.6 ± 0.3

Gaussian + exponential:

$\langle x\rangle$	-5.9 ± 0.2
σ	127.0 ± 0.2
τ	1.58 ± 0.01

TABLE I: Fit parameters

Fitting with both function was done for different p bins in the interval 3 – 20 GeV/c. Width of bins was 0.5 GeV/c below 10 GeV/c and 1.0 GeV/c elsewehere. For both function, resolution was fitted with a constant to gain the overall resolution through all momentum bins. For Gaussian + exponential, shown at Fig. 10, resolution $\sigma/\sqrt{2} = 86.1 \pm 0.2$ ps while for Gaussian only, shown at Fig. 11, it is $\sigma/\sqrt{2} = 88.1 \pm 0.2$ ps. As can be observed from those plots, time resolution is stable through the selected interval of momentum.

While fitting with Gaussian + exponential, we have one more parameter (τ) than in the simple Gaussian fit. To have

[2]Time of start of the collision can be obtained from T0 or directly from TOF if the collision has sufficient multiplicity.

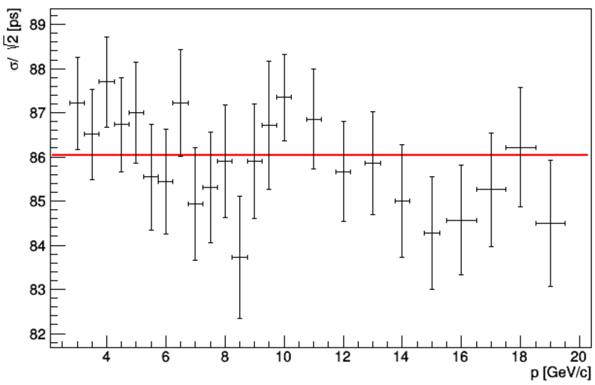

Fig. 10: Time resolution for different momentum bins obtained from fitting $t_{\mathrm{TOF}} - {}^{L}/{}_{c}$ with a Gaussian + exponential.

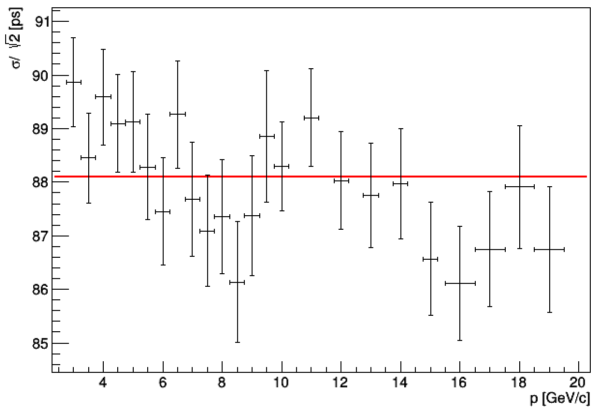

Fig. 11: Time resolution for different momentum bins obtained from fitting $t_{\mathrm{TOF}} - {}^{L}/{}_{c}$ with a Gaussian.

a predicted shape of the tail, we expect the value of τ to be close to 1. Fitting value of τ in the interval 3 – 20 GeV/c for different p bins with a constant, we obtained $\tau = 1.59 \pm 0.01$. Values and the fit are shown on Fig. 12.

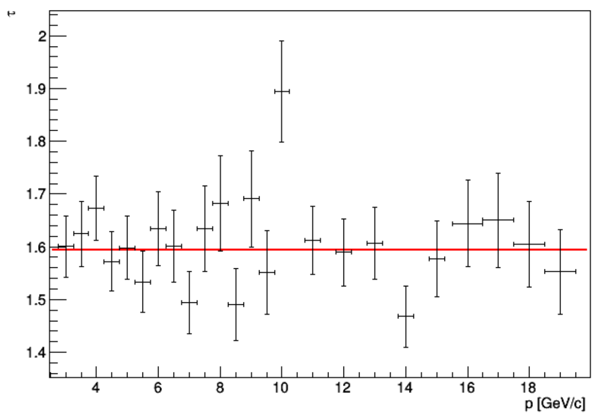

Fig. 12: τ for different momentum bins obtained from fitting $t_{\mathrm{TOF}} - {}^{L}/{}_{c}$ with a Gaussian + exponential.

Since we proved that the time resolution is not depending on the momentum (at least within the interval 3–20 GeV/c), the next step was to check the uniformity with different levels of granularity of TOF detector. It is important to say that we are highly limited by the lack of statistics. This is strongly biased by hits in TOF, shown at Fig. 13. Cosmic particles are coming mostly from the top (around sector 4, numeration is shown on Fig. 14) and escaping at the bottom (sec. 13). On the sides of the detector (sec. 0, 8, 9, 17), we have just few hits, so the statistics is not sufficient to obtain the time resolution there.

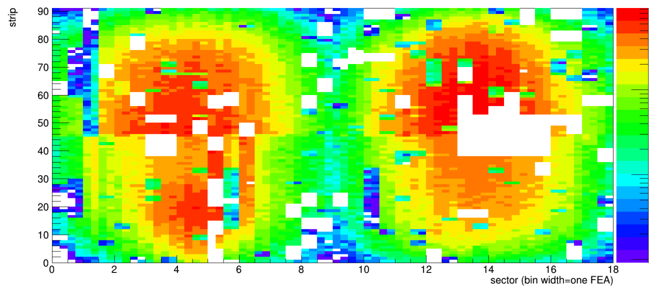

Fig. 13: Map of hits in TOF. Sector = SM, strip = MRPC. No hits in sectors 13-15 are caused by PHOS calorimeter (no strips in TOF).

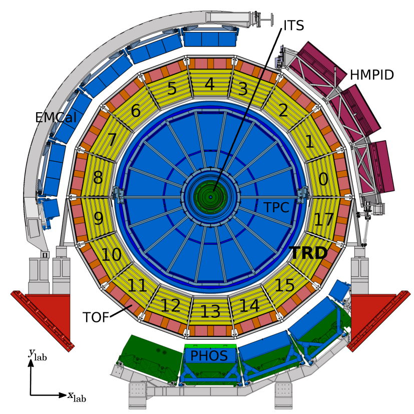

Fig. 14: Numeration of TOF supermodules (sectors).

The first level of granularity observed was division of TOF by its geometry, so to supermodules (sectors). As mentioned in chapter I, each SM contains 15-19 strips. If there were more than 150 different hits per strip, the histogram of $t_{\mathrm{TOF}} - {}^{L}/{}_{c}$ was fitted with a Gaussian. The resolution shown on Fig. 15 was obtained as ${}^{\sigma}/{}_{\sqrt{2}}$. As one can see, the time resolution is stable over all sectors (with sufficient statistics, so except few entries in sector 8 or 17). The mean value is ~ 90 ps.

Every sector can be further divided into 4 front-end analytics (FEA). Present statistics is insufficient for gaining the time resolution at this level of granularity. However, we can observe different levels, namely TRM (TDC readout module). As in previous case, for each TRM, the distribution of $t_{\mathrm{TOF}} - {}^{L}/{}_{c}$ was fitted with a Gaussian. Obtained resolution is shown on Fig. 16. Except for the central part, which needs to be further examined, the resolution is stable with the mean value ~ 90 ps.

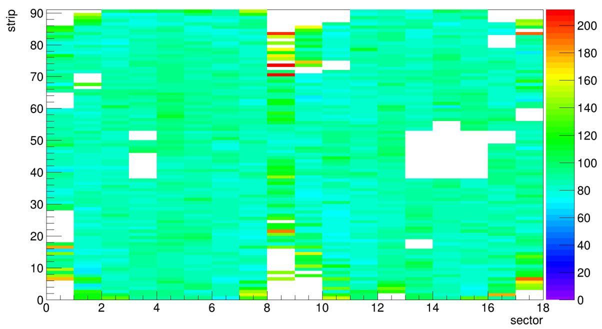

Fig. 15: Resolution for sectors × strips, resolution on z axis is in ps.

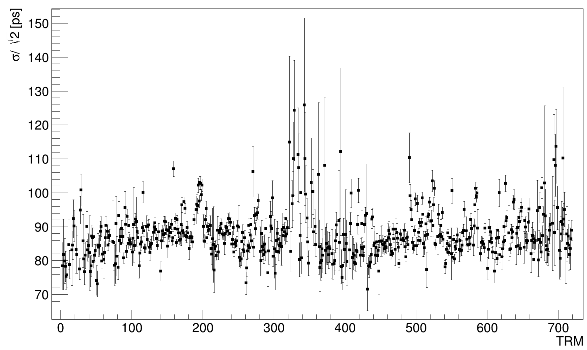

Fig. 16: Resolution for TRM (TDC readout module).

V. Closure test with pp data

As a final step, an analysis on pp data at $\sqrt{s} = 13$ TeV from Run 2 was performed to check the obtained resolution. Only the tracks meeting the criteria $p > 0.5$ GeV/c and hit in TOF were used. The distribution of $t_{\mathrm{TOF}} = t'_{\mathrm{TOF}} - t_{\mathrm{start}} - t_{\mathrm{exp}}$ is shown at Fig. 17, where t'_{TOF} is the time recorded by TOF, t_{start} is start time obtained from TOF and t_{exp} is the time expected for a pion with a corresponding momentum to hit the TOF. Only events with more than 60 tracks were considered since the resolution of the starting time from TOF is a function of multiplicity.

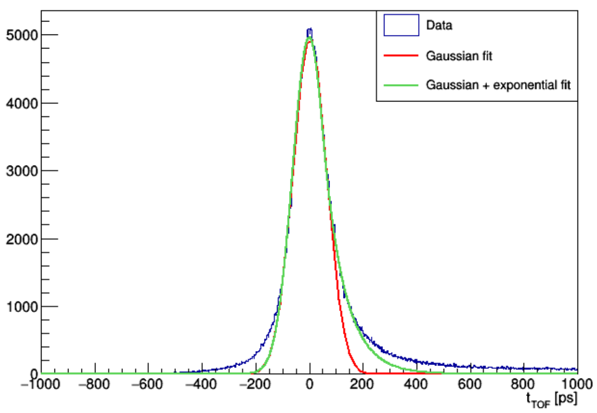

Fig. 17: Distribution of t_{TOF}.

From fitting the distribution at the Fig. 17 with the Gaussian and with the Gaussian + exponential function, σ parameter was obtained with values (62.7 ± 0.3) ps and (62.0 ± 0.2) ps, respectively. The resolution of t_{start} at chosen multiplicity is $\sim$ 20 ps [1], which makes the resolution of TOF $\sim$ 58 ps, therefore in the very good accordance with already published results.

VI. Conclusion

To have the good particle identification capabilities, the ALICE Time-Of-Flight detector needs to have a good time resolution stable through different levels of granularity. Time resolution of 56 ps is derived from beam data. To check the stability, analysis of cosmic rays was performed. Chosen events were very clear with two tracks only (one cosmic muon). The time resolution, obtained as $\sigma/\sqrt{2}$, where σ was obtained by fitting the $t_{\mathrm{TOF}} - L/c$ distribution with a Gaussian, is $\sim$ 90 ps. The stability was checked for different momentum bins in the interval 3 – 20 GeV/c, for geometry division of TOF (sectors × strips) and for TRM (TDC readout module). Further division (till single channel level) was not possible because of lack of statistics.

References

[1] F. Carnesecchi. *Performance of the ALICE Time-Of-Flight detector at the LHC*, arXiv:1806.03825
[2] M. Sitta. *Cosmic-ray studies with ALICE.* ALICE week 2018.